A Simple Model for Rotating Detonation Rocket Engine Sizing and Performance Estimates

Daniel E. Paxson[1] and Hugh D. Perkins[2]
NASA Glenn Research Center, Cleveland, Ohio, 44135, USA

A Rotating Detonation Rocket Engine (RDRE) model is described which characterizes the device as an essentially infinite number of circumferentially arranged, sequentially firing pulse detonation engine (PDE) tubes. The PDE tubes are in turn treated as lumped-parameter chambers, each of which executes a dynamic (i.e. time dependent) Atkinson cycle with an allowance for a finite Mach number during the refill portion of the cycle. The formulation results in several free parameters which are used to essentially tune the model such that it closely matches higher fidelity computational fluid dynamic RDRE simulations in terms of performance, flow rates, etc. The simplicity of the model allows for straightforward combination with component models (e.g. turbopumps, cooling jackets, etc.) as well as implementation within larger vehicle simulations. Such capability allows for realistic mission analyses and benefits studies which will help to determine the best application for the RDRE concept.

Nomenclature

A	=	non-dimensional cross-sectional area
a	=	non-dimensional speed of sound
c_p	=	fuel specific heat
D_m	=	mean diameter
F_{sp}	=	non-dimensional specific thrust
g_c	=	gravitational acceleration
H_m	=	equilibrium mixture enthalpy
H_p	=	equilibrium product enthalpy
h_f	=	fuel heating value
I_{sp}	=	specific impulse
L	=	length
o/f	=	oxidizer-to-fuel mass ratio
P	=	non-dimensional pressure
Pr	=	Prandtl number
$\dot{Q}$	=	total heat transfer rate into walls
q_0	=	non-dimensional mixture heating value
R_g	=	real gas constant
T	=	non-dimensional temperature
u	=	non-dimensional circumferential-component velocity
u_{det}	=	non-dimensional detonation velocity
v	=	non-dimensional axial-component velocity
$\dot{W}$	=	specific work
w	=	non-dimensional mass flow rate

[1] Aerospace Research Engineer, Research and Engineering Directorate, AIAA Associate Fellow.
[2] Aerospace Research Engineer, Research and Engineering Directorate, AIAA Senior Member

x = non-dimensional circumferential direction
y = non-dimensional axial direction

Greek
β = heat transfer parameter
δ = channel height
γ = ratio of specific heats
ρ = non-dimensional density
τ = non-dimensional time
μ = fluid viscosity

Subscripts
a = actual
c = chamber
cv = constant volume
cy = cycle
e = exit plane
eff = effective
$fuel$ = pertaining to the liquid fuel
gg = gas generator
i = ideal
in = inlet
$final$ = end of the refill process
m = inlet manifold
$mean$ = mean value between liquid fuel inlet and outlet
0 = ambient
p = pump
$refill$ = refilling portion of a cycle
t = total
th = throat
$wall$ = RDRE material wall

Superscripts
$*$ = reference value

Overbar
$\hat{}$ = dimensional variable
$\bar{}$ = average

I. Introduction

The pressure gain combustion (PGC) community is currently investigating the concept of rotating detonation rocket engines (RDRE) for space propulsion. If successful, RDRE's could lead to highly compact propulsion systems that deliver high specific impulse at substantially lower pump discharge pressure when compared to conventional rocket engines. The RDRE essentially consists of an annulus with one end open (or having a throat and/or nozzle) and the other end valved (typically using non-mechanical, fluidic means). Fuel and oxidizer enter axially through the valved end. The detonation travels circumferentially. Combustion products exit predominantly axially through the open end. A majority of the fluid entering the device is passed over by the rotating detonation wave which, as a form of confined heat release, substantially raises the pressure and temperature. The fluid is then expanded and accelerated as it travels down the annulus. Detailed descriptions of operation are abundant in the literature (e.g., Refs. 1 and 2). In principle, the flow exiting the device has a higher average total pressure than the flow that enters. Mechanically, RDRE's are relatively simple. Fluidically, they are remarkably complex. There are multiple length and time scales to consider along with multiple fluid states. As such, it is expected that successful designs will require extensive high-fidelity computational fluid dynamic (CFD) studies and validating experiments to reach fruition [1]. Due to the highly coupled nature of these devices and the difficulties associated with instrumentation, it is also expected that performance optimization will necessitate exercising multi-dimensional, multi-phase, CFD simulations of complete RDRE's over numerous parametric variations.

In order to motivate such work however, there exists a need for much simpler models that can compute the performance, flow rates, and physical dimensions of a presumably successful RDRE design. These can be subsequently integrated into larger vehicle system models to assess benefits and requirements for a variety of missions. The work described in this paper represents a preliminary effort at filling this need.

Basic thermodynamic models have been developed that estimate ideal performance [3, 4]. However, they cannot answer questions about sizing, or heat transfer. Furthermore, their idealizations do not account for several fundamental losses (sources of entropy production that are inherent in the RDRE cycle). As such, their predictions are impossibly ideal.

A more sophisticated thermodynamic model has been developed which uses time-dependent sub-models with parameters that were tuned to match CFD simulations [5]. This model produces realistic performance and sizing information. However, many of its empirical coefficients are based on CFD simulations of rotating detonation engine (RDE) configurations intended for airbreathing applications. Furthermore, the formulation does not lend itself to adding critical component models such as cooling channels. The present effort is aimed at rocket applications with only the most basic dimensions required to characterize a given configuration. As such, a simpler, more generic approach than that of Ref. 5 is in order.

In this paper, a model is described that characterizes the RDRE as an essentially infinite number of circumferentially arranged, sequentially firing pulse detonation engine (PDE) tubes. The PDE tubes are in turn treated as lumped-parameter chambers, each of which has a valve at the inlet and a throat at the exit. Each chamber executes a dynamic (i.e. time dependent) Atkinson cycle with an allowance for finite inflow Mach number as it refills. This formulation results in several free parameters that are used to tune the model such that it closely matches an experimentally validated, high fidelity, computational fluid dynamic (CFD) RDRE simulation [2, 6, 7]. The model has been implemented as Visual Basic code in a spreadsheet which can compute a converged cycle in under 1 second on a modern laptop computer. The governing equations and assumptions will be described, followed by a presentation of preliminary results. Several simple component models will then be described and added to the model to demonstrate the versatility of the present approach. The paper closes with some plans for future work that will allow this model, when embedded in a larger full system or vehicle model, to provide reasonable assessment of RDRE benefits for various missions.

II. Model Description

The model equations for each of the many chambers comprising the RDRE analogous device are based on the assumption of a calorically perfect gas (CPG). The gas constant, R_g is determined from the unreacted fuel and oxidizer combination chosen. The ratio of specific heats, γ is found using a method described below in Subsection A. The complete cycle is divided into three stages: instantaneous constant volume heat release (i.e. combustion), chamber blowdown, and chamber refill. The use of a constant volume combustion process instead of a detonative one is justified by the fact that the availability produced by the two processes is similar [3, 8]; however, only the constant volume process produces a uniform post combustion state throughout the notional chamber, which is essential to the application of a lumped volume treatment [8]. The present model assumes an ideal inlet valve that closes instantaneously at the commencement of combustion and opens fully (without aerodynamic loss) at the commencement of refill.

The post constant volume combustion state may be described using the following relationships.

$$T_{c\_cv} = T_{tm} + \gamma(\gamma - 1)q_0; \ \frac{P_{c\_cv}}{P_{c\_final}} = \frac{T_{c\_cv}}{T_{tm}}; \tag{1}$$

$$q_0 = \frac{h_f}{\gamma R_g \hat{T}^*(1 + o/f)} \tag{2}$$

Here and elsewhere in the paper, normalized (i.e., non-dimensional) variables are the default. Dimensional variables are denoted with a circumflex. Temperature, pressure, and density are normalized by reference values $\hat{T}^*$, $\hat{P}^*$, and $\hat{\rho}^*$. Velocity is normalized by the reference speed of sound, $\hat{a}^*$. In the above equations T_{tm} is the total temperature of the chamber inlet manifold, P_{c_final} is the chamber final pressure at the end of the refill process (discussed below), and *o/f* is the ratio of oxidizer to fuel by mass. Since P_{c_final} is not known at the beginning of a cycle simulation, it is estimated as being equal to the inlet manifold pressure, P_{tm}. The density at any time is found using the non-dimensional equation of state, written as follows.

$$P = \rho T \quad (3)$$

After the instantaneous reaction takes place, the chamber begins a blowdown process governed by time dependent continuity and energy equations.

$$\frac{d\rho_c}{d\tau} = -\rho_{th} v_{th} A_{th} \quad (4)$$

$$\frac{dP_c}{d\tau} = -\gamma\left(T_c \rho_{th} v_{th} A_{th} + \beta\{\rho_{th} v_{th}\}^{0.8}[T_c - T_{wall}]\right) \quad (5)$$

The subscript *th* in these equations refers to a notional throat at the exit of the chamber. The throat is followed by a fixed, expanding nozzle with a user defined expansion ratio. Properties in the nozzle are governed by standard area-Mach number relationships [9]. The nozzle operates in a quasi-steady fashion in the sense that it stores no mass. The flow properties in the exit plane are instantaneously determined by those at the throat, along with the specified ambient pressure and exit area. The throat area is normalized by a reference area, $\hat{A}^*$. The time, τ is normalized by an acoustic transit time defined as the effective chamber length, L_{eff} divided by $\hat{a}^*$. The physical meaning of L_{eff} is presented in Subsection C. The second expression on the right side of Eq. 5 is a wall heat transfer term that depends on a user defined chamber wall temperature, T_{wall} and a geometric and fluid property parameter, β [10] which is also discussed in Subsection C. Equations 4 and 5 are integrated numerically using a two-step Runge-Kutta procedure until the chamber pressure matches the inlet manifold pressure.

At this point the refill process commences. A new detonable mixture enters through the inlet while the remaining post-detonative gas exits through the nozzle. The fresh mixture and hot gas are assumed to stay separated by an interface, across which the pressure is constant, but the density varies. No heat transfer is assumed during this portion of the cycle. As such, the remaining hot gas in the chamber slowly expands isentropically. As such, only one governing equation is needed (i.e. P/ρ^γ is constant). The governing equation may be written similarly to Eq. 5 as follows.

$$\frac{dP_c}{d\tau} = \gamma\left(T_{tm} \rho_{in} v_{in} - T_c \rho_{th} v_{th} A_{th}\right) \quad (6)$$

The inflow from the manifold to the chamber inlet plane is assumed to be isentropic so that it can be written as a function of P_c alone.

$$\rho_{in} v_{in} = \begin{cases} \sqrt{\frac{2}{\gamma-1}} \frac{P_{tm}}{\sqrt{T_{tm}}} \left(\frac{P_c}{P_{tm}}\right)^{\frac{1}{\gamma}} \sqrt{1 - \left(\frac{P_c}{P_{tm}}\right)^{\frac{\gamma-1}{\gamma}}} & if\ \frac{P_c}{P_{tm}} > \left(\frac{2}{\gamma+1}\right)^{\frac{\gamma}{\gamma-1}} \\ \frac{P_{tm}}{\sqrt{T_{tm}}} \left(\frac{2}{\gamma+1}\right)^{\frac{\gamma+1}{2(\gamma-1)}} & if\ \frac{P_c}{P_{tm}} < \left(\frac{2}{\gamma+1}\right)^{\frac{\gamma}{\gamma-1}} \end{cases} \quad (7)$$

Equation 6 is integrated numerically until the total mass that has flowed from the exit during the fill portion matches the mass of gas that was in the tube when the fill portion began. At this point, the cycle has completed and the chamber pressure, P_{c_final} is recorded. A limit cycle has been reached if the value is the same as that used in Eq. 1. If the two values do not match, the current value is substituted for the previous value and the cycle is repeated. Convergence typically takes only a few cycles, beginning with the estimate that $P_{c\_final} = P_{tm}$. This is illustrated in Fig. 1 which shows the calculated chamber pressure over the 4 cycles required to reach limit cycle behavior. The fuel and oxidizer combination and the boundary conditions for this figure are described in Section B.

Upon convergence, the cycle averaged performance parameters are calculated. The mass flow rate is:

$$w = \frac{P_{c\_final}}{T_{tm}\tau_{cy}} \quad (8)$$

Here, τ_{cy} is the cycle time. The specific thrust is:

$$F_{sp} = \frac{\int_0^{\tau_{cy}} \left(\frac{P_e - P_0}{\gamma} + \rho_e v_e^2\right) d\tau}{\int_0^{\tau_{cy}} (\rho_e v_e) d\tau} \quad (9)$$

In this equation, the subscript e refers to the nozzle exit plane, and the subscript 0 refers to the ambient environment.

It is noted that the fill process described allows for a time varying fill Mach number; however, it implicitly assumes that the flow stagnates in the notional chamber at the inflow static pressure (i.e. there is no pressure recovery). This is justified since the detonation process does not have a mechanism for recovery of dynamic pressure [11].

The notional throat used here is fluidic rather than physical. In idealized Quasi-2-Dimensional (Q2D) CFD simulations of RDE's it is observed that the fluid reaches a sonic velocity somewhere downstream of the top of the detonation, but upstream of the exit plane [2]. The location of this throat in the current work determines the characteristic length, L_{eff}. The value of A_{th} controls the fill Mach number as seen in Eq. 6. For the present work, a value of 0.8 is chosen. This leads to a limit cycle average fill Mach number in the range of 0.7- 0.85. While this may seem high, it is noted that Q2D CFD simulations of RDE's have shown axial Mach numbers just in front of the detonation that range from 0.7 at the base of the detonation to over 1.0 at the top [11].

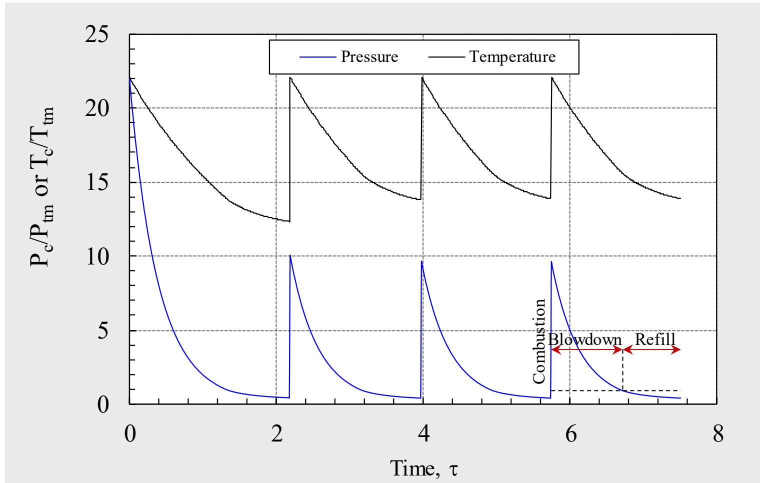

Fig. 1 Chamber pressure and temperature over time as the present model converges to a limit cycle.

A. Ratio of Specific Heats Selection

The ratio of specific heats, γ, can vary substantially in real gases during a detonative cycle. However, in order to use the CPG assumption of this paper only one value can be used. A methodology for selecting this value using the idealized Atkinson cycle may be outlined as follows.

If A_{th} is made very small in the governing equations, the fill Mach number becomes very low. This in turn means that the chamber pressure remains constant at P_{tm} during the refill process. As such, P_{c_final} will not change, and a limit cycle will be achieved in just one cycle. Similarly, the exit conditions at the nozzle also become constant during refill. If the blowdown process is assumed adiabatic (β=0), the time dependency can be eliminated from the Eqns. 4 and 5. As shown in Refs. 12 and 13, the blowdown and refill portions of the ideal Atkinson cycle are described by numerically integrating the chamber properties using discrete density increments. A similar density integral is used to find the specific thrust. With the further simplification of an ideal nozzle this is written as follows.

$$F_{spi} = \frac{-\int_{\rho_{c\_cv}}^{\rho_{c\_refill}} v_e d\rho_c + v_{e\_refill}\rho_{c\_refill}}{\rho_{c\_cv}} \tag{10}$$

The only inputs required are the inlet manifold pressure and temperature, the ambient pressure, and the fuel and oxidizer type and ratio. The exit plane velocity, v_e is a known function of these inputs and the chamber density, ρ_c. This integral is numerically evaluated using the CPG assumption of this paper. The ideal specific thrust integral takes the following form.

$$F_{spi} = \frac{-\sqrt{\left(\frac{2}{\gamma-1}\right)T_{c\_cv}}\left[\int_{\rho_{c\_cv}}^{\rho_{c\_cv}\left(\frac{P_{tm}}{P_{c\_cv}}\right)^{\frac{1}{\gamma}}} \sqrt{\left(\rho_c^{\gamma-1} - \left\{\frac{P_0}{P_{c\_cv}}\right\}^{\frac{\gamma-1}{\gamma}}\right)} d\rho_c - \sqrt{\left(\left\{\frac{P_{tm}}{P_{c\_cv}}\right\}^{\frac{\gamma-1}{\gamma}} - \left\{\frac{P_0}{P_{c\_cv}}\right\}^{\frac{\gamma-1}{\gamma}}\right)}\rho_{c\_cv}\left(\frac{P_{tm}}{P_{c\_cv}}\right)^{\frac{1}{\gamma}}\right]}{\rho_{c\_cv}} \tag{11}$$

Equation 10 can also be evaluated under a multi-species, thermally perfect (i.e. variable γ), equilibrium gas assumption by exercising software designed to compute chemical equilibrium compositions and properties of complex mixtures. An example of such is the CEA (Chemical Equilibrium with Applications) code [14]. This code can compute mixture properties through a constant volume reaction, as well as an isentropic expansion (blowdown). These two processes essentially define the ideal Atkinson cycle. The constant volume reaction provides the post-combustion peak temperature and pressure. The isentropic expansion calculation (initiated with the post-combustion entropy) provides the state of the chamber and the exit plane velocity at incremental densities. This, in turn allows numerical evaluation of Eq. 10.

The value of γ chosen for any operating point in the present work is that for which the ideal specific thrust of the ideal Atkinson cycle calculated via CEA matches that calculated via Eqn. 10. This is an iterative process that involves an initial guess of γ, followed by corrections.

B. Preliminary Results

An adiabatic test (β=0) of the simplified model was made by calculating sea level static specific impulse over a range of manifold pressures and then comparing the values to those from a Q2D CFD RDRE simulation having an ideal inlet with a backflow check valve [5]. The simulation uses the same CPG assumption as the present model. The nozzle expansion ratio of the simplified model was optimized at each manifold pressure. The CFD simulation assumed an ideal nozzle and used the ideal Equivalent Available Pressure (EAP_i) concepts described in Ref. 15 to measure specific impulse. Briefly, this approach ideally expands each element of product mass in the exit plane down to the ambient pressure. From this expansion, an ideal specific (axial) thrust is calculated for each element. An average value is obtained from a mass flux-average of all the elemental specific thrusts.

Unless otherwise stated, all results shown use the properties of premixed RP-1 and gaseous O2 with an equivalence ratio, ϕ=1.3. The relevant parameters are: specific heat ratio, $1.163<\gamma<1.178$; a real gas constant, R_g=47.956 ft-$lb_f/lb_m/R$; and an effective fuel heating value, h_{f_eff}=14.366 BTU/lb_m.

For reference, the effective fuel heating value is an adjusted value that allows rich mixtures to be properly represented with single-gas models. In this work, it is obtained by again exercising the CEA code. CEA is first set up to compute the equilibrium composition and state of a specified fuel and oxidizer mixture at fixed enthalpy and pressure (a so-called hp problem in the CEA terminology). The initial mixture pressure and temperature are required inputs. These are typically 14.7 psia and 540 R, respectively. The relevant output from this calculation is the mixture enthalpy, H_m. CEA is then set up to compute the equilibrium composition and state of the same fuel and oxidizer mixture, fixed at the initial pressure and temperature (a tp problem). The relevant output from this calculation is the product enthalpy, H_p. The effective heating value is then calculated using the following relationship.

$$h_{f\_eff} = \left(H_m - H_p\right)(1 + o/f) \tag{12}$$

The reference state for the preliminary results is: $\hat{P}^*$=14.7 psia, $\hat{\rho}^*$=0.082 lb_m/ft^3, $\hat{T}^*$=540 R, and the corresponding sound speed, $984<\hat{a}^*<991$ ft/s. It is noted that the range in value of the reference sound speed is due to the small change in computed γ as the manifold pressure is changed. Dimensional specific impulse is calculated from non-dimensional specific thrust as follows.

$$I_{sp} = \frac{\hat{a}^* F_{sp}}{g_c} \tag{13}$$

Figure 2 shows the results of the test scenario described. The agreement between the Q2D CFD results and the present model are quite good, lending some measure of confidence to this approach. Contours of temperature in the interior of the unwrapped RDRE annulus as computed by the CFD are shown as an insert for reference. The average fill Mach number from the simplified model is 0.85. The average Mach number in front of the detonation of the CFD simulation is 0.9. Also shown in the figure are results from an ideal Atkinson cycle (i.e. negligible fill Mach, perfect nozzle as described in Section A), and an ideal conventional rocket (constant pressure) calculated with both CEA and with the CPG assumption. It is evident that the CPG assumption is adequate if the proper value of γ is used. It is also evident that the RDRE fill Mach number can cause a substantial decrease in performance compared to an ideal Atkinson cycle. However, even with this deficit, the performance of an RDRE when compared to a conventional engine, is significantly better. Stated another way, it is evident that an RDRE delivers the same performance as a conventional rocket engine at a significantly lower manifold pressure. This could lead to lighter engines with smaller turbopumps, which can be critical for some mission applications.

Practical RDRE's are likely to have a physical throat at their exhaust nozzle entrance, which is known to improve performance [11, 16]. It is possible that the virtual throat, A_{th} in the present work can be correlated to the physical throat which may be present in actual RDRE configurations. This is an activity planned for future versions of this simplified model. However, it is noted that Q2D CFD simulations of semi-ideal RDRE's with physical throats is difficult due to their tendency to develop instabilities [16]. The thermoacoustic-like instabilities are more pronounced

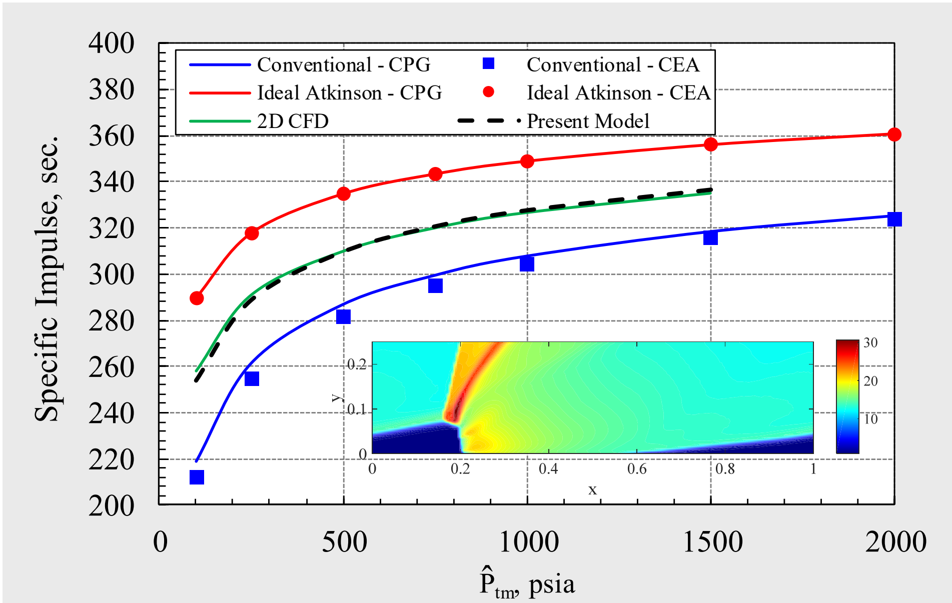

Fig. 2 RDRE specific impulse as a function of manifold pressure for a ϕ=1.3 RP-1/GOX mixture at sea level static conditions using various methods.

with more energetic fuel/oxidizer mixtures such as those found in rockets. They can be mitigated as shown in Ref. 16, but there is a performance cost in doing so. It is not yet known whether the performance enhancement of the throat can outweigh the performance cost of the instability mitigation. It has been shown to do so in less energetic airbreathing RDE's. It is probable that it will also be the case for RDRE's, but to some lesser degree. The conclusion to be drawn from this is that the results of the present model likely represent a lower performance boundary for an idealized RDRE.

C. Sizing and Heat Transfer Modifications

Since the model so far has been described in terms of notional or analogous dimensions there is no way to determine a physical size or an actual thrust from an RDRE. This issue is resolved by supplying a mean diameter, D_m and height, δ for the RDRE annulus. The cycle time is then matched to the time required for a detonation to travel around the annulus. The detonation speed is written as follows [9].

$$u_{det} = \sqrt{(\gamma+1)(\gamma-1)q_0 + 1 + \sqrt{\left((\gamma+1)(\gamma-1)q_0+1\right)^2 - 1}} \tag{14}$$

From the definition of non-dimensional time, the effective chamber length is obtained by:

$$L_{eff} = \frac{\pi D_m}{\tau_{cy} u_{det}} \tag{15}$$

This length is not actually needed for subsequent analysis; however, it does provide a kind of reality check on the lumped volume approach used here. That is, if L_{eff} is on the same order as the sonic choke point seen in validated CFD solutions, then it helps to justify the analysis.

The dimensional mass flow rate is found as follows.

$$\hat{w} = w\hat{\rho}^*\hat{a}^*\pi\delta D_m \tag{16}$$

The heat transfer coefficient in Eq.5 is written as follows.

$$\beta = 0.023\alpha 4\frac{L_{act}}{2\delta}Pr^{-.67}Re^{*-0.2}, \text{where } Re^* = \frac{\hat{\rho}^*\hat{a}^*2\delta}{\bar{\mu}} \tag{17}$$

Here, Pr is the Prandlt number, L_{act} is the actual length of the RDE, $\bar{\mu}$ is the average viscosity of the fluid, and α is a tuning parameter that is used to match the present model with CFD simulation results that were reasonably validated on actual experiments [6, 7, 17]. The essential premises of Eqns. 5 and 17 are that the throat of the lumped volume model supplies density and velocity representative of the entire RDRE, and that the heat flux associated with them occurs along the entire length of the RDRE.

The stoichiometric hydrogen/air RDE experiment used to obtain α is described in Refs. 17 and 18. Two operating points were simulated using the CFD code. The prescribed inlet area of the code was varied until the measured and computed mass flow rates matched using the measured inlet manifold pressures and temperatures. The required code inlet area was 36% greater than the effective area of the experiment, as measured using calibrated cold flow tests. The disparity is consistent with the code assumption of premixed hydrogen and air passing through the inlet when the experiment is actually non-premixed air. Since the density of stoichiometric hydrogen/air is 28% less than pure air, this indicates the code matched the experimental inlet area to within 8%. With this matching, the code predicted thrust to within 15% of measurements and closely matched the two time-averaged internal static pressure measurements, as seen on the right of Fig. 3. The observed detonation height for this rig is approximately 1.0 in. [19] which corresponds to y = 0.11 (non-dimensional axial distance) in the CFD generated temperature contour shown on the left of Fig. 3. This is close to the CFD prediction of y=0.09; again indicating a reasonable agreement.

The present lumped volume model does not yet have a propellant injection sub-model to account for the inevitable pressure drop. It is expected that either liquid or supercritical fuel and oxidizer will be used in RDRE's. Developing an appropriately simplified sub-model that is also compatible with the gaseous assumption of the main model is considered a future task. As such, the present model assumes isentropic flow of a perfect gas through the inlet.

The CFD model does have a sub-model for calculating losses in the inlet, and for the two operating points examined, it predicts an inlet total pressure loss of approximately 50%. When the present lumped volume model was run using the experimental values of D_m (5.7 in.) and δ (0.3 in.), and with the measured manifold pressure debited by 50% (65.84 psia), it predicted the mass flow rate of the experiment to within 5%. It is interesting to note that the present model predicts an effective volume length of 1.48 inches. In the temperature contour of Fig. 3, this corresponds to approximately y=0.165. This is consistent with the aforementioned choke point just downstream of the top of the detonation.

The CFD code predicts that approximately 17% of the available chemical energy is absorbed by the cold walls in this experiment. Considering the results of Ref. 20, this is a reasonable estimate. The value of α in Eq. 14 required to match this heat flux rate is 3.4. With this value of α the lumped volume model prediction of thrust matched the CFD prediction for both operating points to within 5.6%.

III. Results and Discussion

The tuned model was used to predict performance and sizing for an example 190,000 lbf sea level thrust RDRE with an inlet manifold pressure of 1,250 psia. The propellant combination is identical to Fig. 2. A channel inner-to-outer diameter ratio of 0.8 was used. Limits to this critical sizing parameter are not yet established in the community. An optimal value for the actual length to channel hydraulic diameter ratio is also not established. As such, a value of 5 is chosen based on an informal average of experimental rigs described in the literature. This yielded a mean diameter

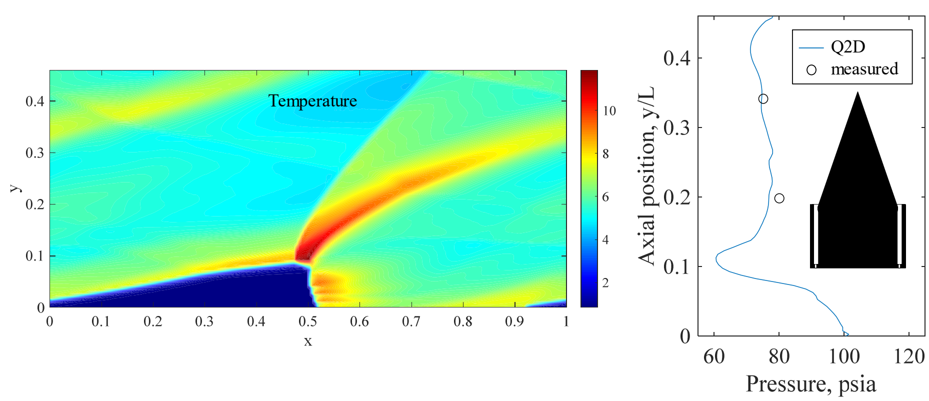

Fig. 3 Q2D CFD simulation of the NPS experiment showing computed contours of temperature on left, and comparison of time averaged pressure on the right for one of the two code validation tests examined.

of 11.80 inches. A wall temperature of 2400 R is specified. Under these conditions and for this sizing, approximately 4%-7% of the chemical energy is absorbed by the cooled walls. The impact on performance is shown in Fig. 4 where specific impulse is plotted as a function of inlet manifold pressure similar to Fig. 2. At the design manifold pressure, the wall heat transfer causes an approximately 3% reduction in specific impulse. While this is significant, the RDRE performance still remains above that of an ideal conventional engine. Furthermore, it is noted that the curve shown is strongly affected by the RDRE length, and the inner-to-outer diameter ratio. Changing the former from 5 to 2.5 times the channel hydraulic diameter, and changing the latter from 0.8 to 0.7, yields a mean diameter of 9.35 in. and a specific impulse loss to heat transfer of only 1.2%. Since it is not clear yet what these critical geometric parameters should be on any theoretical basis, it is reasonable to expect that values lower than those used here can be made practical and yield higher performance.

Of course, these and other parameters cannot be specified in isolation. Figure 5 schematically shows the two configurations just described, but with an optimally sized nozzle added. The expansion ratio for this nozzle was determined by the lumped volume model to be the value that produced the highest specific impulse for the specified manifold inlet pressure and the ambient exhaust pressure. It is apparent that the shorter RDRE has the longer nozzle. Since an actual RDRE will require cooling in both the nozzle and the combustor, it is quite possible that the effect of the reduced heat transfer losses seen in the shorter RDRE will be at least partially washed out by the longer nozzle. Considerations and first order assessments such as this, which are straightforward with the present model, demonstrate its utility.

A. Adding Components

The simplicity of the present model makes the addition of realistic components straightforward. This in turn allows for meaningful comparison with conventional rocket engines. As a first example of this, consider the addition of a gas generator. The gas generator creates hot gas to drive a turbine which then powers turbopumps to deliver fuel and oxidizer to the RDRE. The hot gas is created by conventionally combusting a small fraction of the propellants as a very rich mixture (thereby keeping the temperature relatively low). The gas is sent through the turbine and then overboard. Thus, it does not typically contribute to thrust. The component is modeled here assumes a turbine inlet temperature of 2300 R, a single stage turbine pressure ratio of 3.0, and a turbine efficiency of 0.6. The efficiencies of both the oxidizer and fuel turbopumps are assumed to be 0.9. These specifications along with the tank pressure (assumed 14.7 psia), inlet manifold pressure, and assumed liquid densities of fuel and oxidizer define the specific work available from the turbine, $\dot{W}_{gg}$, and the specific work required by the pumps, $\dot{W}_p$. A simple power balance then yields the following relationship for the gas generator mass flow rate.

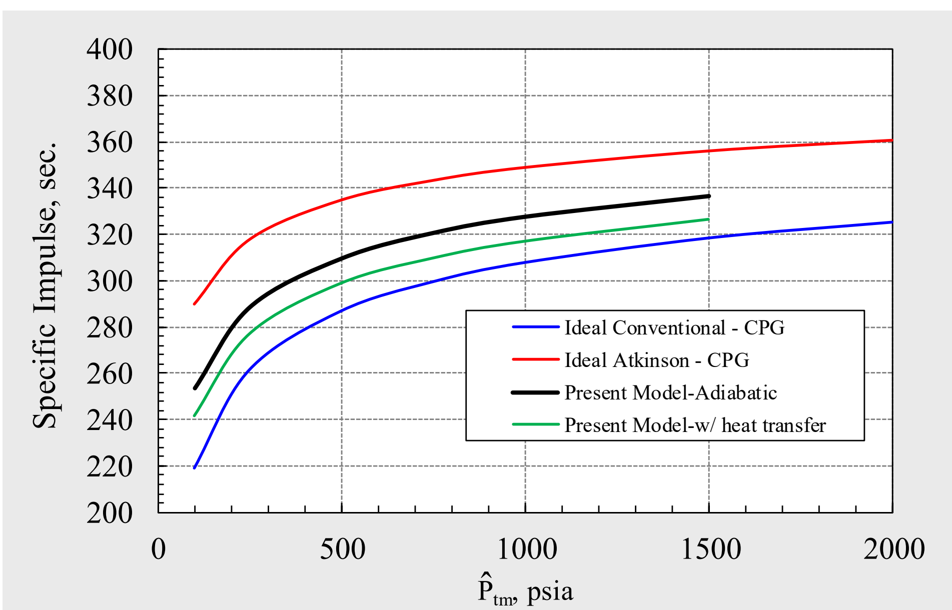

Fig. 4 RDRE specific impulse as a function of manifold pressure for a ϕ=1.3 RP-1/GOX mixture at sea level static conditions for the adiabatic and heat transfer versions of the present lumped volume model.

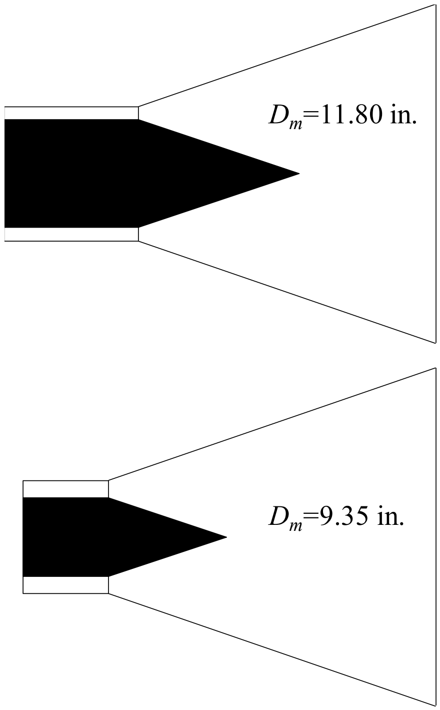

Fig. 5 Notional, scaled RDRE configurations providing similar specific impulse but with differing channel inner-to-outer diameter ratios and chamber length.

$$\hat{w}_{gg} = \hat{w}_{RDRE}\left(\frac{\dot{W}_p}{\dot{W}_{gg}-\dot{W}_p}\right) \tag{18}$$

The subscript RDRE here refers to the propellant that is flowing into the RDRE chamber. It is noted that Eq. 18 is not entirely correct since it assumes that the *o/f* ratio of the gas generator is identical to the RDRE chamber. However, since the amount of propellant going through the gas generator is a small fraction of the total flow, and the current component model is intended to be illustrative, the simplification and resulting error are considered acceptable. The calculation for specific thrust then becomes:

$$F_{sp\_gg} = \frac{F_{sp}}{\left(1+{}^{\hat{w}_{gg}}/_{\hat{w}_{RDRE}}\right)} \tag{19}$$

The performance impact of the gas generator component on the example rocket engine is seen in Fig. 6. It is evident that the impact becomes prohibitive as the manifold pressure increases. There is virtually no increase in specific impulse with manifold pressures above 1000 psia.

As a second example of the present model utility, the issue of RDRE cooling is briefly examined. The focus is on the RDRE proper and does not include the nozzle. Since RDRE's are known to have high heat transfer rates that are associated with the detonation process, there is some question as to whether conventional fuel cooled channels are adequate to thermally protect the walls. Using the example RDRE described above, the heat load to the walls, $\dot{Q}$ is known, as is the fuel flow rate, $\hat{w}_{fuel}$. The heat load is assumed to be split between the annulus outer and inner walls in proportion to their relative surface areas. The heat load must be absorbed by the fuel. The properties of liquid RP-1 are readily obtained as a function of temperature

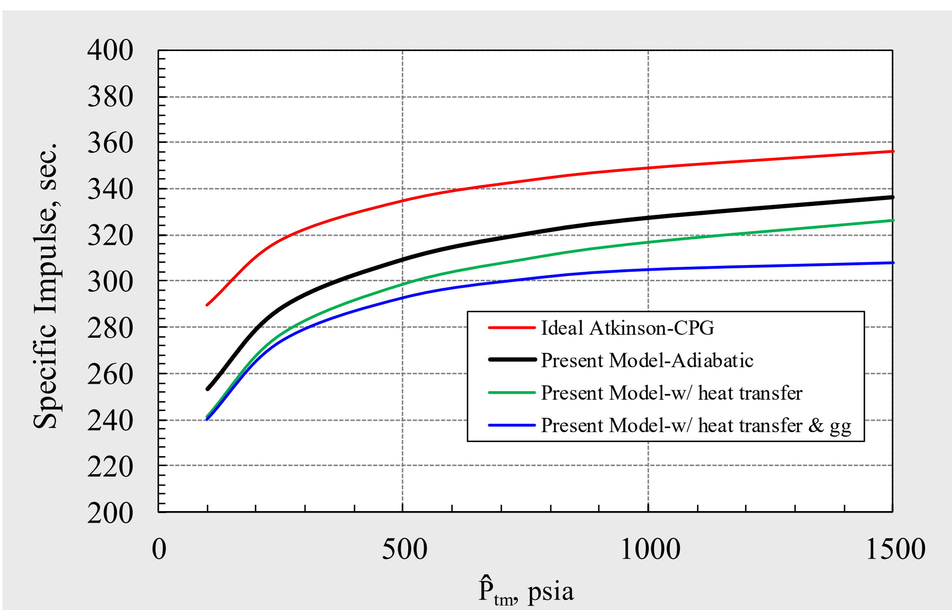

Fig. 6 RDRE specific impulse as a function of manifold pressure for a ϕ=1.3 RP-1/GOX mixture at sea level static conditions for the present lumped volume model with the effects of heat transfer and an added gas generator.

from the literature [21]. The cooling channels are approximately rectangular in cross-section as shown schematically in Fig. 7. It is assumed that 75% of the wetted perimeter is available for heat transfer. Each passage runs the length of the RDRE. The passage walls are assumed to be held uniformly at the specified $\hat{T}_{wall}$. This information is sufficient to calculate a mean fuel coolant temperature, $\hat{T}_{fuel\_mean}$.

$$\hat{T}_{fuel\_mean} = \hat{T}_{fuel\_in} + \frac{\dot{Q}}{2\hat{w}_{fuel}c_p(\hat{T}_{fuel\_mean})} \tag{20}$$

For this example, the temperature of the fuel into the passages was assumed to be $\hat{T}_{fuel\_in}$=520 R. Equation 20 is transcendental because the specific heat is a function of the mean fuel temperature. However, it can easily be solved numerically through recursion. Once the mean temperature is known, the mean density and thermal conductivity, and viscosity are also known via the aforementioned thermodynamic properties. From this point, the modeling process will be described in words, but without mathematical formulae. These are standard [10], but too numerous to be justified for the purposes of this paper.

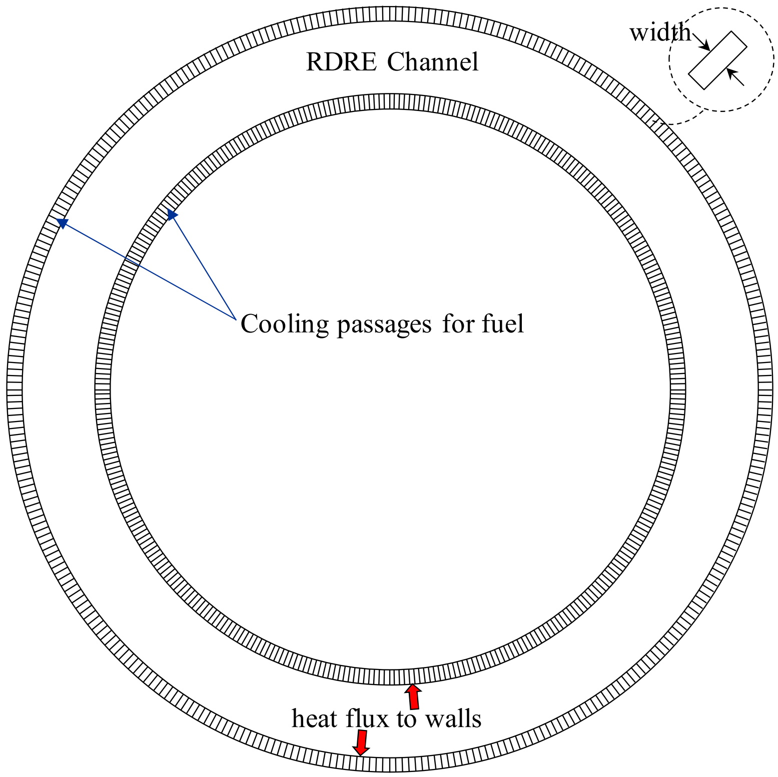

Fig. 7 RDRE cooling passage schematic.

A guess is made at the passage width and aspect ratio. This information allows the calculation of how many passages can fit on the inner and outer annulus diameter. From this, the target heat load per channel which the fuel must absorb can be found. The fuel flow rate per passage is then calculated. This is used with the known passage cross sectional area and mean fuel density to calculate the mean velocity. The velocity, hydraulic diameter, density, and viscosity are then used to calculate a Reynolds number, which together with the Prandtl number can be used with standard empirical correlations to find a Nusselt number. Using the definition of the Nusselt number, the hydraulic diameter, and the thermal conductivity, a heat transfer coefficient is obtained for the inside of the passage. The heat transfer coefficient, inner surface area, and temperature difference between the wall and the fuel yield the actual heat load transferred to the fuel. If this matches the target load, then the initial guess at the passage width was correct. If not, then a new guess is made, and the process is repeated. Numerous root finding (aka, goal seeking) routines can be used to find the correct width iteratively [22]. The final Reynolds number obtained is then used to find a friction factor which, combined with the length and velocity, determines the pressure drop across the cooling passages. If the pressure drop meets a user defined acceptable value, then the initial guess of the aspect ratio was correct. If not, then a new guess is made and the iteration above is repeated. This process can also be iteratively brought to closure.

For the example RDRE described, a pressure drop equal to 20% of the inlet manifold pressure was chosen to be the acceptable limit. This means that the fuel turbopump must do more work, which in turn means reduced specific impulse for a gas generator cycle. However, the impact is negligibly small in the present analysis (an approximate reduction of 0.3%). It was found that with cooling passages of 0.055 in. width (with sidewall thickness of 0.025 in.), having an aspect ratio of 4.3, the cooling requirements could be met. This yielded 755 passages around the outer diameter and 604 passages around the inner diameter. The cooling passage outlet temperature of the fuel was found to be 1635 R, which is likely unacceptably high in terms of coking [23]. It is interesting to note in this regard that the alternative configuration shown at the bottom of Fig. 5 yielded an exit temperature of 1146 R, which is near the acceptable value for RP-1.

Of course, the addition of the present fuel cooling component to the model is not intended to be definitive. It is merely intended to illustrate the utility of the model for considering preliminary RDRE configurations, and for making quantitative benefits assessments more realistic.

IV. Conclusion

A Rotating Detonation Rocket Engine (RDRE) model was presented which analogizes the rotating detonation to an infinite number of circumferentially arranged, sequentially firing, lumped-parameter chambers, each of which executes a time-dependent Atkinson cycle with finite refill Mach number. Adding the requirement that the cycle time for each of the chambers must match the period of rotation for a detonation wave effectively determines the RDRE diameter. The model formulation resulted in several free parameters which were used to match its output to that of higher fidelity computational fluid dynamic RDRE simulations, and experiments. It was demonstrated that real world sub-components can be easily added to the model (e.g. turbopumps, cooling channels), thereby creating a RDRE propulsion system model that can be used for mission analysis and benefits studies. Additional components are planned for a future version of the model including a propellant injector loss sub-model and a nozzle performance sub-model. The goal is to incorporate the result into a full vehicle analysis package that will aid RDRE technology development.

Acknowledgments

The research for this paper was supported by a 2018 NASA Center Innovation Fund award. The experimental validation data for this work was provided by Dr. Christopher M. Brophy, and Dr. Joshua R. Codoni of the Naval Postgraduate School, in Monterey, CA. The authors would like to thank them both for acquiring and sharing it.

References

[1] Lietz, C., Ross, M., Desai, Y., and Hargus, W.A., "Numerical Investigation of Operational Performance in a Methane-Oxygen Rotating Detonation Rocket Engine," AIAA Paper 2020-0687, January 2020.

[2] Paxson, D.E., "Numerical Analysis of a Rotating Detonation Engine in the Relative Reference Frame," AIAA Paper 2014-0284, January 2014, also NASA/TM 2014-216634, 2014.

[3] Heiser, W. H., Pratt, D. T., "Thermodynamic Cycle Analysis of Pulse Detonation Engines", *Journal of Propulsion and Power*, Vol. 18, No. 1, pp 68-76, 2002.

[4] Paulson, E. J., Kimura, R., Hargus, W.A., Sankaran, V., "Ideal Thermodynamic Performance Results for Rotating Detonation Rocket Engine Thrust Chambers Using CEA," AIAA Paper 2020-0193, January 2020.

[5] Kaemming, T.A., Fotia, M.A., Hoke J.L., Schauer, F.R., "Thermodynamic Modeling of a Rotating Detonation Engine Through a Reduced-Order Approach," *AIAA Journal of Propulsion and Power*, V. 33, No. 5, 2017, pp. 1170-1178.

[6] Paxson, D. E., Fotia, M. L., Hoke, J. L., Schauer, F. R., "Comparison of Numerically Simulated and Experimentally Measured Performance of a Rotating Detonation Engine," AIAA Paper 2015-1101, January 2015, also NASA/TM—2015-218835, 2015.

[7] Rankin, B., Fotia, M. L., Paxson, D. E., Hoke, J. L., Schauer, F. R., "Experimental and Numerical Evaluation of Pressure Gain Combustion in a Rotating Detonation Engine," AIAA Paper 2015-0877, January 2015.

[8] Paxson, D. E., Brophy, C., Bruening, G., "Performance Evaluation of a Pulse Detonation Combustion Based Propulsion System Using Multiple Methods," *JANNAF Journal of Propulsion and Energetics*, Vol. 3, No. 1, May 2010, pp 44-55.

[9] Thompson, P.A., *Compressible Fluid Dynamics*, Rensselaer Polytechnic Institute, Troy, NY, 1988, Chapter 5.

[10] Holman, J.P., *Heat Transfer*, McGraw-Hill, New York, 1981, Chapter 6.

[11] Paxson, D. E. "Impact of an Exhaust Throat on Semi-Idealized Rotating Detonation Engine Performance," AIAA-2016-1647, January 2016, also NASA/TM-2016-219076, 2016.

[12] Paxson, D. E., Kaemming, T. A., "Foundational Performance Analyses of Pressure Gain Combustion Thermodynamic Benefits for Gas Turbines," AIAA Paper 2012-0770, January 2012, also NASA/TM-2012-217443.

[13] Paxson, D. E., Kaemming, T. A., "Influence of Unsteadiness on the Analysis of Pressure Gain Combustion Devices," *AIAA Journal of Propulsion and Power*, V. 30, No. 2, 2014, pp. 377-383.

[14] Gordon, S. and McBride, B., "Computer Program for Calculation of Complex Chemical Equilibrium Compositions and Applications," NASA RP-1311, Oct 1994.

[15] Kaemming, T. A., Paxson, D. E., "Determining the Pressure Gain of Pressure Gain Combustion," AIAA Paper 2018-4567, July, 2018.

[16] Paxson, D. E., Schwer, D. A., "Operational Stability Limits in Rotating Detonation Engine Numerical Simulations," AIAA Paper 2019-0748, January 2019.

[17] Miki, K. Paxson, D.E., Perkins, H.D., Yungster, S., "RDE Nozzle Computational Design Methodology Development and Application," AIAA Paper 2020-3872, August 2020.

[18] Brophy, C. M., Codoni, J.R., Teneyck, J. A., Spencer, E., "Experimental performance characterization of an RDE using Equivalent Available Pressure," AIAA Paper 2019-4212, August 2019.

[19] Dausen, D.F., Brophy, C. M., Wright, R. G., Marder, J. D., "Design of an Optically-Accessible Rotating Detonation Engine," AIAA Paper 2012-3944 August 2012.
[20] Theuerkauf, S. W., Schauer, F. R., Anthony, R. J., Paxson, D. E., Stevens, C. A. Hoke, J. L., "Comparison of Simulated and Measured Instantaneous Heat Flux in a Rotating Detonation Engine," AIAA Paper 2016-1200, January 2016.
[21] Outcalt, S. L., Laesecke, A., Brumback, K. J., "Thermophysical Properties Measurements of Rocket Propellants RP-1 and RP-2," *AIAA Journal of Propulsion and Power*, V. 25, No. 5, 2009, pp. 1032-1040.
[22] Press, W.H., Teukolsky, S.A., Vetterling, W.T., Flannery, B.P., *Numerical Recipes: The Art of Scientific Computing*, Cambridge University Press, Cambridge, 1986, Chapter 9.
[23] Roback, R., et al, "Deposit Formation in Hydrocarbon Rocket Fuels," NASA CR-165405, August, 1981.